

# **FLUX-VECTOR SPLITTING FOR UNSTEADY CALCULATIONS ON DYNAMIC MESHES**

W. Kyle Anderson  
James L. Thomas  
Christopher L. Rumsey  
NASA Langley Research Center

PRECEDING PAGE BLANK NOT FILMED

The method of flux-vector-splitting used in the current study is that of Van Leer<sup>1</sup>. The fluxes split in this manner have the advantage of being continuously differentiable at eigenvalue sign changes and this allows normal shocks to be captured with at most two interior zones, although in practice only one zone is usually observed. The fluxes as originally derived, however did not include the necessary terms appropriate for calculations on a dynamic mesh. The extension of the splitting to include these terms while retaining the advantages of the original splitting is the main purpose of the present investigation. In addition, the use of multiple grids to reduce the computer time is investigated. A subiterative procedure to eliminate factorization and linearization errors so that larger time steps can be used is also investigated.

## PURPOSE

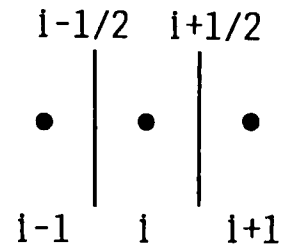
- Extend the Van Leer method of flux vector splitting for use on moving meshes
- Investigate the use of multiple grids to reduce computer time
- Use of multigrid with a sub-iterative procedure to eliminate factorization and linearization errors

The upwind differencing in the present work is achieved through the technique of flux-vector-splitting where the fluxes are split into forward and backward contributions according to the signs of the eigenvalues of the Jacobian matrices, and differenced accordingly. The split-flux differences are implemented as a flux balance across a cell corresponding to MUSCL (Monotone Upstream-Centered Schemes for Conservation Laws) type differencing<sup>2</sup>. Here, the fluxes at each cell interface are formed from the metric terms at the cell interface, and the state variables are obtained by upwind-biased interpolation of the conserved variables.

## FLUX VECTOR SPLITTING

- Split fluxes into forward and backward contributions  

$$F(Q) = F^+(Q^-) + F^-(Q^+)$$
- Use upwind biased approximation to spatial derivatives
- Van Leer splitting
  - Continuously differentiable
  - Allows shocks to be captured with at most two (usually one) interior zones



In order to facilitate the derivation of the split fluxes, it is convenient to revert to the one-dimensional Euler equations on a moving grid. The one dimensional Euler equations express the conservation of mass, momentum, and energy for an inviscid, nonconducting gas in the absence of external forces. The flux is written as a function of the density, speed of sound, local Mach number relative to the moving grid, and the mesh speed.

## ONE DIMENSIONAL EULER EQUATIONS

$$\hat{F}(\rho, a, M; \hat{\xi}_t) = \left\{ \begin{array}{l} \rho a M \\ \rho a^2 \left( M^2 + \frac{1}{\gamma} - \frac{\hat{\xi}_t M}{a} \right) \\ \rho a^3 \left( \frac{M}{\gamma-1} + \frac{M^3}{2} - \frac{M^2 \hat{\xi}_t}{a} + \frac{\hat{\xi}_t^2 M}{2a^2} - \frac{\hat{\xi}_t}{\gamma a} \right) \end{array} \right\}$$

$$M = \frac{U + \hat{\xi}_t}{a} = \text{Mach number relative to moving grid}$$

In deriving the splittings for a dynamic mesh, several requirements are placed on the split fluxes: these requirements are identical to those originally imposed by Van Leer for the fixed grid equations, with an additional constraint requiring simply that for zero grid speed the split fluxes revert to those for a stationary grid. Eight requirements are ultimately placed on the split fluxes of which the five most important ones are shown.

## REQUIREMENTS FOR VAN LEER SPLITTINGS

- $\hat{F}(\hat{Q}; \hat{\xi}_t) = \hat{F}^+(\hat{Q}; \hat{\xi}_t) + \hat{F}^-(\hat{Q}; \hat{\xi}_t)$
- $\partial \hat{F}^+ / \partial \hat{Q}$  must have all eigenvalues  $\geq 0$   
 $\partial \hat{F}^- / \partial \hat{Q}$  must have all eigenvalues  $\leq 0$
- $\partial \hat{F}^\pm / \partial \hat{Q}$  must be continuous
- $\partial \hat{F}^\pm / \partial \hat{Q}$  must have one eigenvalue vanish for subsonic Mach numbers
- $\hat{F}^+(\hat{Q}; \hat{\xi}_t) = \hat{F}(\hat{Q}; \hat{\xi}_t)$  for  $M \geq 1$   
 $\hat{F}^-(\hat{Q}; \hat{\xi}_t) = \hat{F}(\hat{Q}; \hat{\xi}_t)$  for  $M \leq -1$

With the Mach number defined relative to the grid, the mass flux has the same form as that of the fixed grid equations. Therefore the splitting of the mass flux for a moving grid is the same as for the fixed grid equations. The momentum flux is split in a similar fashion.

## SPLITTING THE FLUX VECTORS

- Mass flux has identical form as for a stationary grid

$$f_1^{\pm}(\rho, a, M) = \pm \frac{\rho a}{4} [M \pm 1]^2$$

- Momentum flux

$$f_2^{\pm}(\rho, a, M; \hat{\xi}_t) = f_1^{\pm} a \left[ \frac{\gamma-1}{\gamma} M \pm \frac{2}{\gamma} - \frac{\hat{\xi}_t}{a} \right]$$

The formation of the energy flux can now be obtained from a combination of the split mass and momentum fluxes. The formation of the energy flux in this manner insures its degeneracy, thereby guaranteeing shock structures with no more than two interior zones.

## SPLITTING THE FLUX VECTORS

- Energy flux formed from combination of mass and momentum fluxes ensures degeneracy

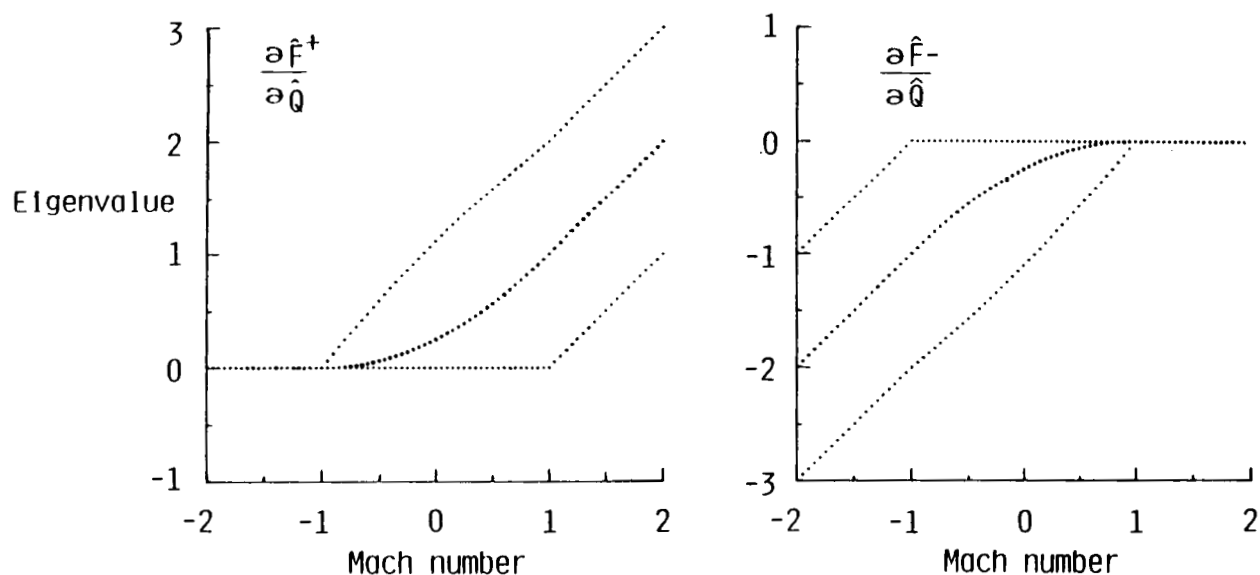
$$f_3^\pm(f_1, f_2; \hat{\xi}_t) = c_1 \frac{(f_2^\pm)^2}{f_1^\pm} + c_2 f_2^\pm \hat{\xi}_t + c_3 f_1^\pm \hat{\xi}_t^2$$

$$c_1 = \frac{\gamma^2}{2(\gamma^2-1)} \quad c_2 = \frac{1}{\gamma^2-1} \quad c_3 = \frac{1}{2(\gamma^2-1)}$$

- Degenerate flux guarantees shock structures with no more than two interior zones (generally one)

The eigenvalues of the Jacobians of the split fluxes are shown for an exemplary grid speed. All eigenvalues of  $F^+$  are non-negative while all the eigenvalues of  $F^-$  are non-positive. In addition, each has one eigenvalue vanishing for subsonic Mach numbers. The differentiability of the fluxes is also indicated in the figure since the eigenvalues are representative of the derivatives of the fluxes in canonical form and all are continuous over the Mach number range.

### EIGENVALUES OF $\partial \hat{F}^\pm / \partial \hat{Q}$ ( $\hat{\xi}_t = 0.5$ )





The method used to advance the solution in time is an implicit finite volume method<sup>3</sup>. Since implicit methods allow much larger time steps than explicit methods, the allowable time step is dictated more by the physics of the flow than by stability considerations. The scheme can be either first or second order accurate in time and either first, second or third order accurate in space. Since upwind differencing is employed, no explicitly added artificial viscosity is needed and is therefore not used.

## **TIME ADVANCEMENT ALGORITHM**

- Backward time implicit algorithm
  - Approximate factorization
  - First or second order time accurate
- Finite volume implementation
- No explicitly added artificial viscosity
- Explicit boundary conditions

The basic algorithm utilizes approximate factorization to obtain the solution at each time step. For three dimensions the algorithm is implemented in three steps, one for each spatial direction. Using first order spatial differencing on the implicit side of the equation, the scheme requires the solution of a system of block tridiagonal equations in each coordinate direction and is completely vectorizable since the operations in each factor are independent of the other two. For unsteady calculations, several sub-iterations can be used at each time step to eliminate unwanted factorization and linearization errors.

### THREE-DIMENSIONAL ALGORITHM

$$\left[ \left( I + \frac{\Phi}{2} \right) + \Delta t \sigma_{\xi}^{-} \hat{A}^{+} + \Delta t \sigma_{\xi}^{+} \hat{A}^{-} \right] \Delta \hat{Q}^{*} = -\Delta t L(\hat{Q}^{\mathcal{Q}})$$

$$\left[ \left( I + \frac{\Phi}{2} \right) + \Delta t \sigma_{\eta}^{-} \hat{B}^{+} + \Delta t \sigma_{\eta}^{+} \hat{B}^{-} \right] \Delta \hat{Q}^{**} = \left[ I + \frac{\Phi}{2} \right] \Delta \hat{Q}^{*}$$

$$\left[ \left( I + \frac{\Phi}{2} \right) + \Delta t \sigma_{\zeta}^{-} \hat{C}^{+} + \Delta t \sigma_{\zeta}^{+} \hat{C}^{-} \right] \Delta \hat{Q}^{\mathcal{Q}} = \left[ I + \frac{\Phi}{2} \right] \Delta \hat{Q}^{**}$$

$$\hat{Q}^{\mathcal{Q}+1} = \hat{Q}^{\mathcal{Q}} + \Delta \hat{Q}^{\mathcal{Q}}$$

$$\Phi = 0 \quad \text{first order time}$$

$$\Phi = 1 \quad \text{second order time}$$

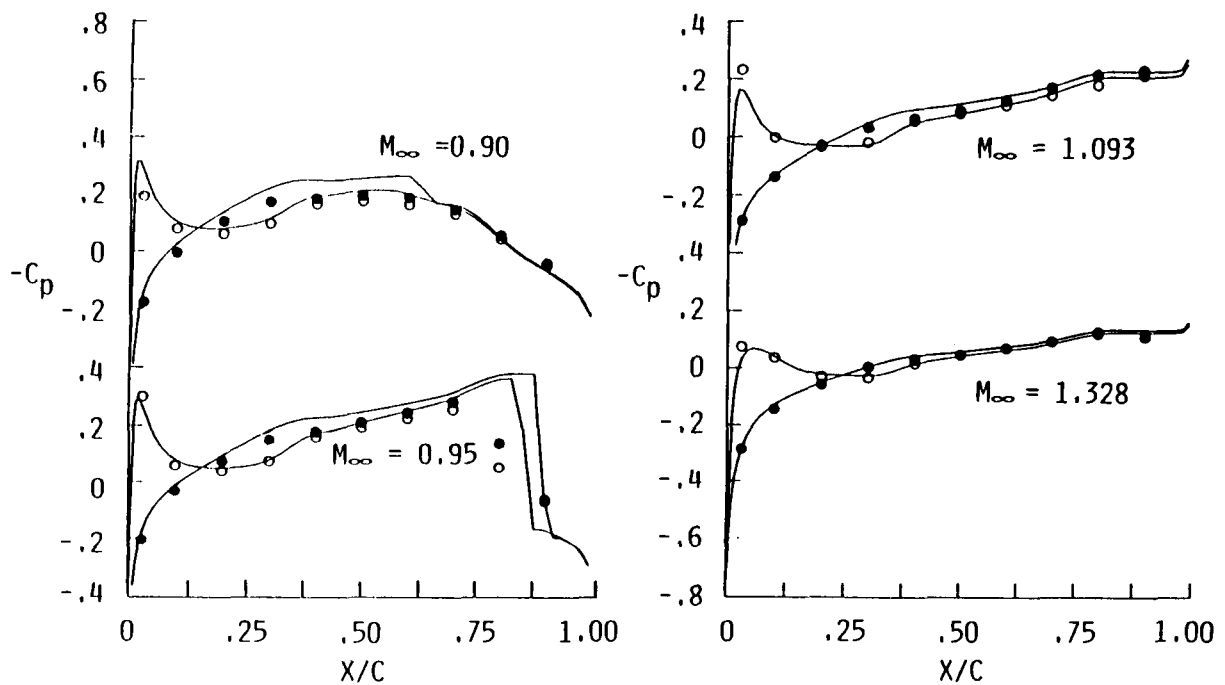
Steady computations are compared with experiment for the F-5 fighter wing at four freestream Mach numbers and an angle of attack of zero degrees. The mesh used in the computations is a  $129 \times 33 \times 33$  C-H mesh corresponding to 129 points along the airfoil and wake, 33 points approximately normal to the airfoil, and 33 points in the spanwise direction, 17 of which are on the wing planform. For each Mach number, an inboard and outboard span station are shown, corresponding to  $y/s=0.174$  and  $y/s=0.8412$ , respectively where  $y$  is the coordinate in the spanwise direction and  $s$  is the wing semi-span. The results are generally in good agreement with the experimental data at both span stations for all Mach numbers.

### F-5 STEADY PRESSURE DISTRIBUTIONS

$\alpha = 0^\circ$   $y/s = 0.1740$

— Theory  $129 \times 33 \times 33$

○ Experiment

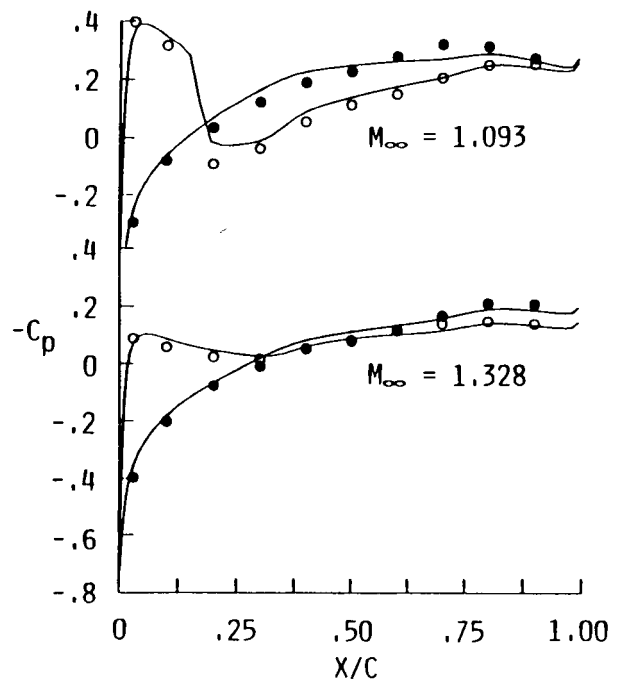
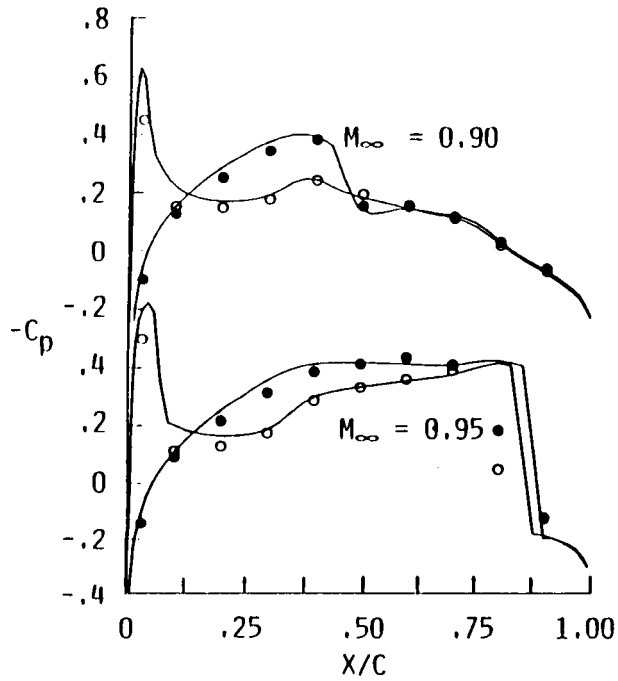


# F-5 STEADY PRESSURE DISTRIBUTIONS

$$\alpha = 0^\circ \quad y/s = 0.8412$$

— Theory 129x33x33

○ Experiment

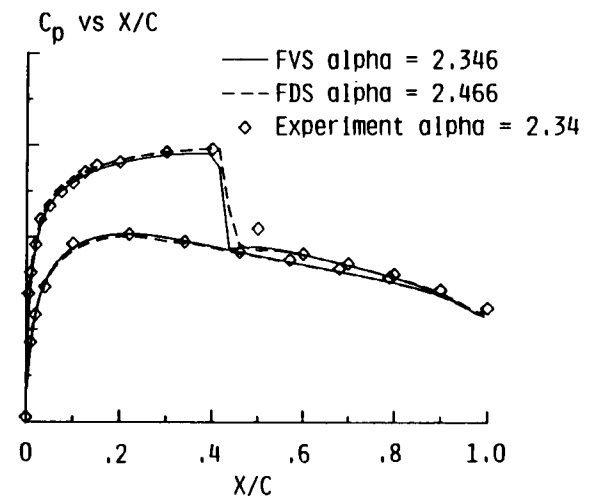
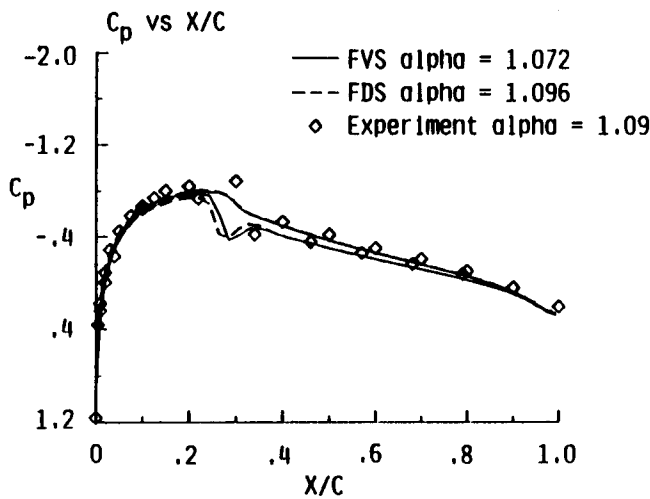


Computational results using both flux-vector-splitting and flux-difference-splitting<sup>4</sup> are compared with experimental data for an NACA 0012 airfoil undergoing forced pitching oscillations. The freestream Mach number is 0.755, the reduced frequency is 0.1628 (based on chord), and the mean and dynamic angles of attack are 0.016 and 2.51 degrees respectively. The results were obtained on a  $193 \times 33$  C-grid using a time step of 0.10 requiring approximately 500 time steps to compute each pitching cycle. The computed pressures using both flux-vector-splitting and flux-difference-splitting compare well with the experiment at all angles of attack in the cycle shown. The shocks are all captured very sharply with no oscillations. Results for the negative angles of attack are similar.

### UNSTEADY PRESSURE DISTRIBUTION

NACA 0012  $M_\infty = 0.755$   $k = 0.1628$

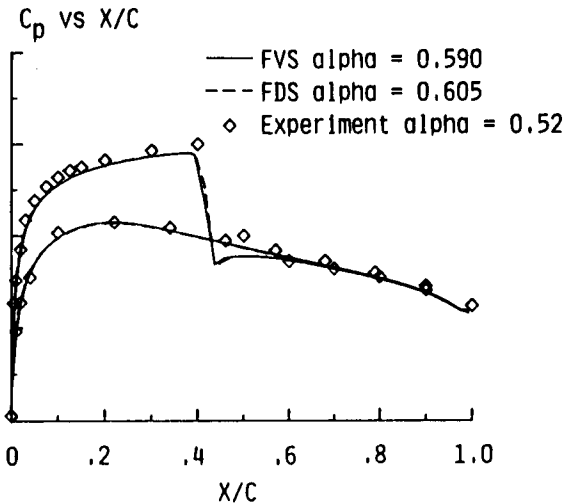
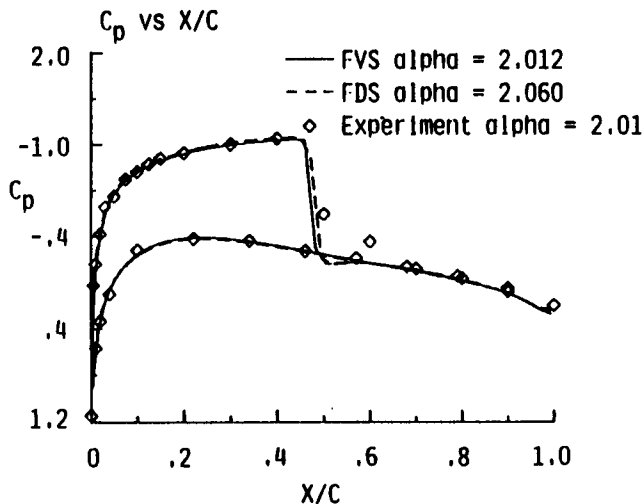
$\alpha_0 = 0.016$   $\alpha_1 = 2.51$



### UNSTEADY PRESSURE DISTRIBUTION

NACA 0012  $M_\infty = 0.755$   $k = 0.1628$

$\alpha_0 = 0.016$   $\alpha_1 = 2.51$



Although the time step allowed by the implicit method is much larger than that allowed by explicit methods, the time steps used may still be relatively small so that resolving the motion requires extensive computational effort, especially for three-dimensional flows where the number of grid points used in the discretization of the flowfield may be large. The multiple grid method has proven to be effective in reducing the computational work for steady flows, although little work has been done for unsteady flows. Jespersen<sup>5</sup> has shown that the multigrid concept could be used to advance the solution in time on coarser meshes while maintaining first order accuracy in time. The impetus is in reducing the computer time by performing some of the calculations on coarser meshes where fewer operations are required.

## NONITERATIVE USE OF MULTIPLE GRID LEVELS

- Advance solution on coarser grids where computations are inexpensive
- Addition of relative truncation error between fine grid and coarser grid maintains high order spatial accuracy

$$M_1(\hat{Q}_1^{n+1} - \hat{Q}_1^n) = -\Delta t [\hat{L}_1(\hat{Q}_1^n) - \tau_1]$$

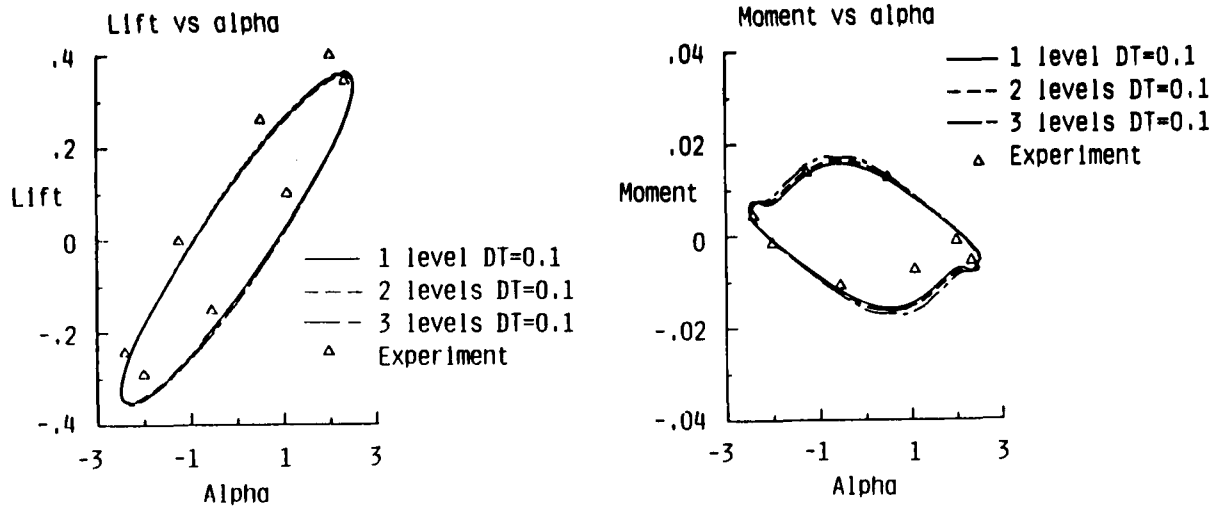
- First order temporal accuracy

Results are shown comparing calculated lift and moment coefficients against experimental data for the pitching NACA 0012 airfoil previously described. Also shown in the figure are results obtained using the noniterative multiple grid technique for the time accurate calculations. The lift and moment calculations are in excellent agreement between the single level and two level cases. With three levels, however, the pitching moment exhibits slightly larger disagreement with the single level results.

### UNSTEADY FORCES AND MOMENTS

NACA 0012  $M_\infty = 0.755$   $k = 0.1628$

$\alpha_0 = 0.016$   $\alpha_1 = 2.51$

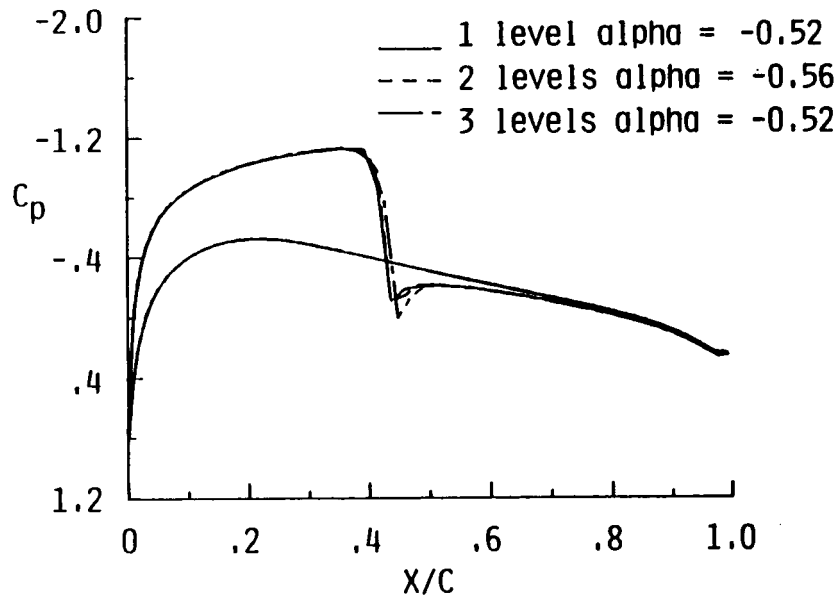


Pressure results are shown at one point in the pitching cycle when one, two, and three grids are used. As seen, the pressure distributions between the single level and two level cases are virtually indistinguishable; the pressures obtained using three grid levels, however, differ somewhat from the other two, particularly at the base of the shock. The explanation for this lies partly in the fact that each of the coarse grids is influenced strongly by the residual on the finest grid. Therefore, as the number of grid levels is increased, the residual which is driving the problem has been evaluated at an earlier point in the cycle. When only two grids are employed, the residual on the fine grid can be evaluated at the correct angle of attack in the cycle so that no lag in the residual exists.

## PRESSURE DISTRIBUTION FOR SINGLE AND MULTIPLE GRIDS

NACA 0012  $M_\infty = 0.755$   $k = 0.1628$

$\alpha_0 = 0.016$   $\alpha_1 = 2.51$





Results indicate that the use of multiple grids can give reasonably accurate results while decreasing the computer time. Use of more than two grid levels, however, leads to increasing errors.

## **NONITERATIVE USE OF MULTIPLE GRID LEVELS**

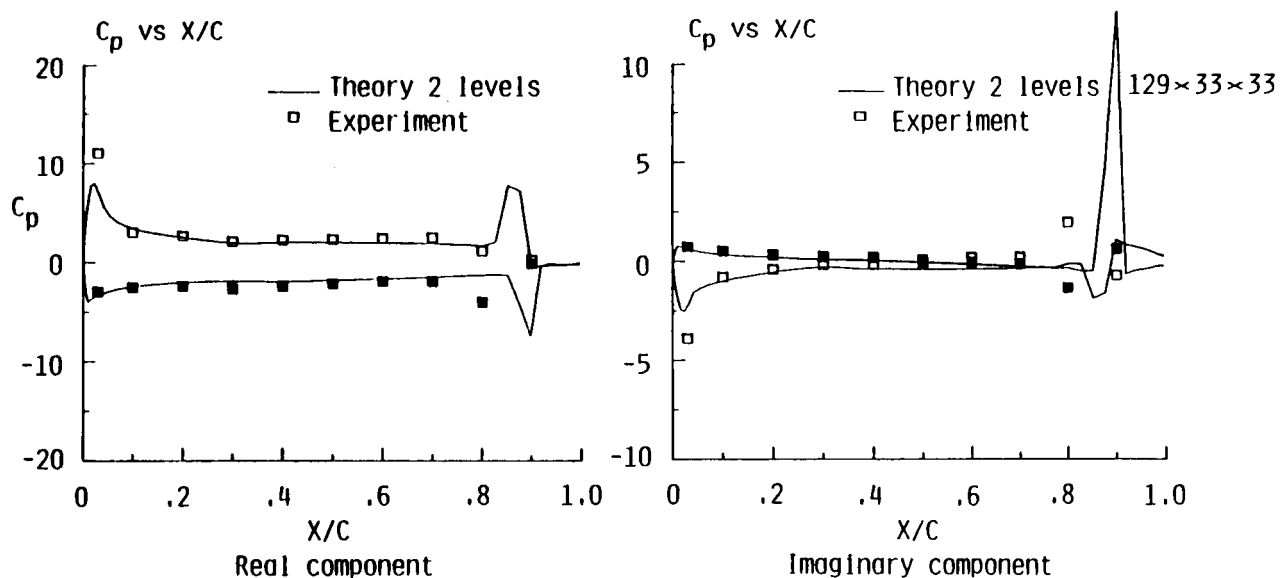
- Solution using two grid levels are virtually identical to single grid solution
- Two time steps are taken with only a slight increase in cost over a single step
- Use of more than two grids leads to increasing errors

Unsteady results for the F-5 wing are compared with experiment at a freestream Mach number of 0.95 undergoing forced pitching motion where the mean angle of attack is zero degrees, the unsteady amplitude is 0.532 degrees, and the reduced frequency based on root chord is 0.264. The results have been computed on a  $129 \times 33 \times 33$  mesh using two grid levels and a time step of 0.05 on each grid requiring approximately 250 fine grid time steps per pitching cycle. The real and imaginary components of the pressure coefficients are compared with experiment at two span stations. As before, the results show reasonable comparison with experiment. However, the characteristic pressure spike at the shock is somewhat aft of the experimental results indicating that viscous effects may be important.

### UNSTEADY PRESSURE FOR F-5 WING

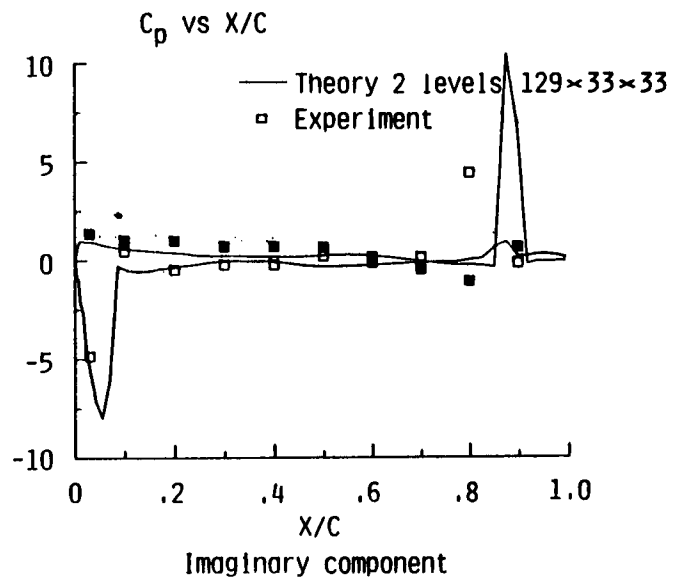
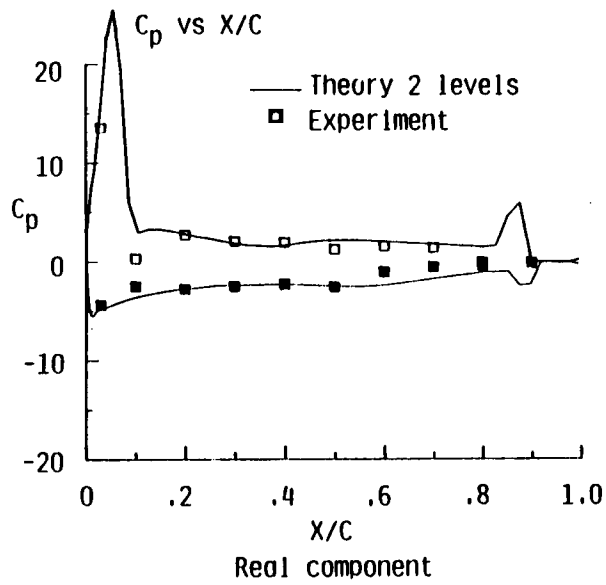
$$M_\infty = 0.95 \quad k = 0.264 \quad \alpha_0 = 0 \quad \alpha_1 = 0.532$$

$$y/s = 0.1740$$



# UNSTEADY PRESSURE FOR F-5 WING

$M_\infty = 0.95$   $k = 0.264$   $\alpha_0 = 0$   $\alpha_1 = 0.532$   
 $y/s = 0.8412$



At each time step, several iterations of the algorithm may be carried out in order to eliminate factorization and linearization errors. These subiterations may be done using a multigrid method to accelerate the convergence at each time step. The benefits of the subiterations are observed to be generally offset by the extra computational work required at each time step.

## ITERATIVE MULTIGRID ALGORITHM

$$M (\hat{Q}^{l+1} - \hat{Q}^l) = -\Delta t L(Q^l)$$

- Repeated iterations at each time step will eliminate factorization and linearization errors so larger time steps can be taken
- Use of multigrid method accelerates convergence
- Benefits of larger time step generally offset by extra computational work
- May be more beneficial for incomplete linearizations or with "frozen" flux Jacobians

## CONCLUSIONS

- Van Leer method of flux vector splitting extended for use on dynamic grids
- Use of coarser grids result in substantial reduction of computer time with virtually no loss in accuracy
- Use of multigrid to eliminate factorization and linearization error only marginally beneficial
- Results compare favorably with experiment for two and three dimensional test cases

## References

1. Van Leer, B.: Flux Vector Splitting for Euler Equations. Lecture Notes in Physics, Vol. 170, 1982, pp. 501-512.
2. Van Leer, B.: Towards the Ultimate Conservative Difference Scheme V., A Second Order Sequel to Gudonov's Method. Journal of Computational Physics, Vol. 32, 1979 pp. 101-136.
3. Anderson, W.K., Thomas, J.L., and Rumsey, C.L., Extension and Application of Flux-Vector-Splitting to Unsteady Calculations on Dynamic Meshes. AIAA 87-1152-CP, Presented at 8<sup>th</sup> Computational Fluid Dynamics Conference, June 9-11, Honolulu, Hawaii.
4. Roe, P.L.: Approximate Riemann Solvers, Parameter Vectors, and Difference Schemes. Journal of Computational Physics, Vol. 43, 1981 pp. 357-372.
5. Jespersen, D.C.: A Time-Accurate Multiple Grid Algorithm. AIAA 85-1493, July 1985.